Hindawi
Journal of Applied Mathematics
Volume 2023, Article ID 1902844, 13 pages
https://doi.org/10.1155/2023/1902844

Research Article

Hydromagnetic Flow of Two Immiscible Couple Stress Fluids through Porous Medium in a Cylindrical Pipe with Slip Effect

Punnamchandar Bitla[1] **and Yitagesu Daba Kore**[2]

[1]*Department of Mathematics, Anurag University, Telangana, India*
[2]*Department of Mathematics, Wollega University, Nekemte, Ethiopia*

Correspondence should be addressed to Punnamchandar Bitla; punnam.nitw@gmail.com

Received 23 November 2022; Revised 23 February 2023; Accepted 18 April 2023; Published 3 May 2023

Academic Editor: Oluwole D. Makinde

In this study, the steady hydromagnetic flow of two immiscible couple stress fluids through a uniform porous medium in a cylindrical pipe with slip effect is investigated analytically. Essentially, the flow system is divided into two regions, region I and region II, which occupy the core and periphery of the system, respectively. The flow is driven by a constant pressure gradient applied in a direction parallel to the cylinder's axis, and an external uniform magnetic field is applied in the direction perpendicular to the direction of fluid motion. Instead of the classical no-slip condition, the slip velocity along with vanishing couple stress boundary conditions is taken on the surface of the rigid cylinder, and continuity conditions of velocity, vorticity, shear stress, and couple stress are imposed at the fluid-fluid interface. The governing equations are modeled using the fully developed flow conditions. The resulting differential equations governing the flow in the two regions are converted to nondimensional forms using appropriate dimensionless variables. The nondimensional equations are solved analytically, and closed-form expressions for the flow velocity, flow rate, and stresses are derived in terms of the Bessel functions. The impacts of several parameters pertaining to the flow such as the magnetic number, couple stress parameters, Darcy number, viscosity ratio, Reynolds number, and slip parameter on the velocities in respective regions are examined and illustrated through graphs. The flow rate's numerical values are also calculated for different fluid parameters and displayed in tabular form. It is found that increasing the magnetic number, viscosity ratio, Reynolds number, and slip parameters decreases the velocities of the fluids whereas increasing the couple stress parameter, Darcy number, and pressure gradient increases fluid velocities. The results obtained in this paper show an excellent agreement with the already existing results in the literature as limiting cases.

1. Introduction

Over the last few decades, the study of non-Newtonian fluids has received a lot of attention as these types of fluids frequently occur in many industrial, scientific, and technological processes. Many important complex and real fluids which include molten metals, polymeric liquids, slurries, blood, liquid crystals, lubricants, soaps, greases, gelatin, and paints belong to this family of fluids. This class of fluids does not follow the Newtonian fluid theory as they possess microstructure and a nonsymmetric stress tensor in their fluid structure. For this reason, several new microcontinuum theories [1–3] pertaining to non-Newtonian fluids have been developed for describing the rheological behavior of numerous complex fluids. The couple stress fluid, initiated by stokes [4], is one of the popular theories of polar fluids that considers the possibility of polar effects such as the presence of couple stresses and body couples in the fluid medium. The flow behavior of various fluids that contain a substructure such as lubricants with small amounts of additives, polymers, colloidal suspensions, liquid crystals, animal and human blood, polymer-thickened oils, muddy water, and electrorheological and synthetic fluids can be modeled using the couple stress fluid theory [5]. A couple stress fluid model has been successfully employed to study the mechanism of peristalsis [6, 7]. The couple stress fluid theory widely used in modeling the flow of biological fluids such as synovial fluids [8–11] and blood [12–14].

In realistic situations, most of the flow problems arising in the industries, manufacturing process, geology, groundwater hydrology, reservoir mechanics, biomechanics, magnetofluid dynamics, geophysics, plasma physics, and so on occur with two or more fluids of different densities/viscosities flowing immiscibly in the same channel or cylindrical pipe. Examples of these systems are the flow of several immiscible oils through the bed of rocks or soils, the flow in the rivers with several industrial fluids, blood flow in the arteries, the flow of air and fuel droplets in combustion chambers, the flow of air and exhaust gases at engine outlets, gas and Petrolia flow in pipes of oil, water-air flows around ship halts, etc. These are referred to as multiphase flows in the literature. Owing to its wide areas of applications, several researchers have studied multiphase fluid flows. Chaturani and Samy [15] as well as Sinha and Singh [16] investigated the effects of couple stresses on blood flow, and many other authors (Valanis and Sun [17], Sharan and Popel [18], and Garcia and Riahi [19]) discussed blood flow considering it as a two-phase flow in which they have assumed blood as a couple stress fluid. Besides its application in blood flow, the study of multiphase flow has several important applications in various fields of engineering and science. Umavathi et al. [20] analytically solved the problem of flow through a horizontal channel with a couple stress fluid sandwiched between viscous fluid layers. They discussed the effects of various flow parameters and concluded that the couple stress parameter influences the flow. Umavathi et al. [21] made a detailed study on the flow and heat transfer of a couple stress fluid in contact with a Newtonian fluid. Abbas et al. [22] analyzed the hydromagnetic mixed convective two-phase flow of couple stress and viscous fluids in an inclined channel. They obtained closed-form solutions of velocity and temperature profiles by using the perturbation method. Devakar et al. [23] studied the unsteady flow of couple stress fluid sandwiched between Newtonian fluids through a channel. There are many other works concerning multiphase fluid flows (see Packham and Shall [24], Rao and Usha [25], Chamkha et. al [26], Umavathi et al. [27, 28], and Umavathi and Shekar [29]).

In view of its numerous applications, the researchers at present are engaged in exploring immiscible flows of fluids through a porous medium under various circumstances. Umavathi et al. [30] studied the problem of the convective flow of two immiscible fluids (couple stress and viscous fluids) through a vertical channel. They obtained an approximate solution by using the regular perturbation method. Devakar and Ramgopal [31] presented analytical solutions for the fully developed flows of two immiscible couple stress and Newtonian fluids through a nonporous and porous medium in a horizontal cylinder. Srinivas and Murthy [32] studied the flow of two immiscible couple stress fluids between two permeable beds. They obtained an exact solution to the considered problem. An analysis of the Poiseuille flow of immiscible micropolar-Newtonian fluids through concentric pipes filled with the porous medium was done by Yadav et al. [33]. Other important studies in this direction include Chamkha [34], Harmindar and Singh [35], Singh [36], and Srinivas et al. [37]. Though many researchers have worked on the flow of immiscible fluids through porous channels, the flow of immiscible non-Newtonian fluids through porous cylinders is reasonably underexplored despite its applicability in blood flows, chemical engineering, crude oil extraction, etc. One such type of problem is going to be discussed in this paper.

Magnetohydrodynamics (MHD) is also an interesting and important area of modern engineering sciences and involves the interaction of magnetic forces and electrically conducting fluids. The application of magnetic fields to the flow of immiscible fluids originates from reducing the flows for many medical and industrial purposes. The study of the hydromagnetic flow of moving fluids through a porous medium is currently a subject of great interest owing to plentiful applications in industrial, engineering, and medical devices. Owing to these applications, several studies have been conducted to examine the effect of magnetic fields on the flows of immiscible fluids. In light of this, Vajravelu et al. [38] studied the hydromagnetic unsteady flow of two conducting immiscible fluids between two permeable beds. Malashetty et al. [39] analyzed the magnetohydrodynamic two-fluid convective flow and heat transfer in an inclined composite porous medium. Raju and Nagavalli [40] studied the unsteady two-layered fluid flow and heat transfer of conducting fluids in a channel between parallel porous plates under a transverse magnetic field. Ansari and Deo [41] investigated the effect of a magnetic field on the two immiscible viscous fluids flowing in a channel filled with a porous medium. The influence of an inclined magnetic field on the Poiseuille flow of immiscible micropolar-Newtonian fluids through the horizontal porous channel where the permeability of both the regions of the horizontal porous channel has been taken differently was discussed by Yadav and Jaiswal [42]. In another paper, Jaiswal and Yadav [43] investigated the influence of a magnetic field on the Poiseuille flow of immiscible Newtonian fluids through a highly porous medium. More recently, Kumar and Agrawal [44] studied the magnetohydrodynamic pulsatile flow and heat transfer of two immiscible couple stress fluids in a porous channel.

A majority of the studies regarding the flow of immiscible non-Newtonian fluids quoted above were carried out by imposing the no-slip boundary condition. However, several theoretical and experimental studies [45–50] reveal that slip exists at the solid boundary. So, for flows containing fluids through solid boundaries, consideration of a velocity slip is more realistic and appropriate. Recently, Punnamchandar and Fekadu [51] investigated the effects of slip and uniform magnetic field on the flow of immiscible couple stress fluids in a porous medium channel. In another paper, Punnamchandar and Fekadu [52] considered the problem of the effects of slip and inclined magnetic field on the flow of immiscible fluids (couple stress fluid and Jeffrey fluid) in a porous channel. It is observed that the effects of slip and magnetic field on the flow of immiscible couple stress fluids through a porous medium in a cylindrical pipe have not been discussed yet.

Keeping this in view the wide potential applications of immiscible couple stress fluids flow and the importance of exact solutions described above, the goal of the current paper is to determine exact solutions for the steady hydromagnetic flow of two immiscible couple stress fluids through a porous medium in a cylindrical pipe with slip effect. The impacts of different flow parameters on the velocity field and flow rate are investigated. The slip factor in fluid flows makes the problem even more realistic and interesting, which motivated us to consider this problem. The practicality and the complexities involved due to the porosity and cylindrical nature of the geometry also make the work presented in this paper novel.

2. Basic Equations

The basic equations describing the flow of couple stress fluid including a Lorentz force are (Stokes [4, 5]) as follows:

Continuity equation (conservation of mass):

$$\frac{\partial \rho}{\partial t} + \nabla . \left(\rho \vec{q} \right) = 0. \tag{1}$$

Momentum equation (conservation of momentum):

$$\rho \frac{D\vec{q}}{Dt} = \rho \vec{f} + \frac{1}{2} \nabla \times \left(\rho \vec{c} \right) - \nabla P - \mu \nabla \times \nabla \times \vec{q} - \eta \nabla \times \nabla \times \nabla \times \nabla \times \vec{q} + (\lambda + \mu) \nabla \left(\nabla \cdot \vec{q} \right) + \vec{J} \times \vec{B}, \tag{2}$$

where the scalar quantity ρ is the couple stress fluid density and P is the fluid pressure at any point. The vectors q, f, and c are the velocity, body force per unit mass, and body couple per unit mass, respectively. The term $\vec{J} \times \vec{B}$ in equation (2) is the Lorentz force (electromagnetic body force) in which $\vec{J}$ is the electric current density and $\vec{B}$ is the total magnetic field.

The force stress tensor τ_{ij} (Stokes [5]) that arises in the theory of couple stress fluids is given by

$$\tau_{ij} = \left(-P + \lambda \nabla . \vec{q} \right) \delta_{ij} + 2\mu d_{ij} + \frac{1}{2} \varepsilon_{ijk} [m_{,k} + 4\eta \omega_{k,rr} + \rho c_k]. \tag{3}$$

The couple stress tensor m_{ij} (Stokes [5]) that arises in the theory has the linear constitutive relation

$$m_{ij} = \frac{1}{3} m \delta_{ij} + 4\eta' \omega_{j,i} + 4\eta \omega_{i,j}. \tag{4}$$

In the above, $\omega_{i,j}$ is the spin tensor, ρc_k is the body couple vector, d_{ij} is the components of the rate of shear strain, δ_{ij} is the Kronecker symbol, e_{ijk} is the Levi-Civita symbol, and comma denotes covariant differentiation.

The material constants λ and μ are the viscosity coefficients, and η and η' are the couple stress viscosity coefficients satisfying the constraints

$$\mu \geq 0, 3\lambda + 2\mu \geq 0, |\eta| \geq \eta', \eta' \geq 0. \tag{5}$$

There is a length parameter $l = \sqrt{\eta / \mu}$ which is a characteristic measure of the polarity of the couple stress fluid, and this parameter is identically zero in the case of nonpolar fluids.

3. Formulation of the Problem

The physical model concerns an axisymmetric fully developed hydromagnetic flow of two immiscible couple stress fluids flowing through a porous medium in a horizontal circular pipe of radius R_0. Owing to the fluids' immiscibility, there are two separate regions of fluid flow: region I, or the core region, and region II, or the periphery region. The flow geometry of the problem is depicted in a cylindrical polar coordinate system (r, θ, z) with the origin at the center of the tube and common axis of the cylindrical regions taken as the z-axis, as shown in Figure 1. Region I $(0 \leq r \leq R)$ is occupied with couple stress fluid with density ρ_1, shear viscosity μ_1, and couple stress viscosity η_1, comprising the core region of the pipe whereas region II $(R \leq r \leq R_0)$ is occupied by a different couple stress fluid having density ρ_2, shear viscosity μ_2, and couple stress viscosity η_2, comprising the peripheral region of the pipe. The motion of the fluids in both regions is caused by a constant pressure gradient applied in a direction parallel to the cylinder's axis, i.e., z-axis, and an external uniform magnetic field of strength B_0 directed perpendicular to the flow direction is also applied.

To develop the governing equations for the considered model, the following presumptions are taken in the analysis of the current study:

(i) The fluids are considered incompressible, and the flow is assumed to be steady, laminar, and fully developed

(ii) Both the fluid regions are saturated with the uniform porous media of permeability k

(iii) The Lorentz force is the only body force acting on the fluids, with no body couples

(iv) The magnetic Reynolds number of the flow is assumed to be very small, and no external voltage is applied so that the induced magnetic field is neglected and the Hall effect of magnetohydrodynamics is assumed to be negligible

Under the assumptions made, the vector forms of conservation equations governing the flow of steady, incompressible immiscible couple stress fluids through a porous cylinder in the presence of a transverse magnetic field can be written in the following form (Punnamchandar and Fekadu [51] and Kumar and Agrawal [44]):

Continuity equations:

$$\nabla.\vec{q}_i = 0. \tag{6}$$

Momentum equations:

$$\begin{aligned} -\nabla P - \mu_i \nabla \times \nabla \times \vec{q}_i - \eta_i \nabla \times \nabla \times \nabla \times \nabla \\ \times \vec{q}_i + \vec{J}_i \times \vec{B} - \frac{\mu}{k} \vec{q}_i = 0, \end{aligned} \tag{7}$$

where $i = 1, 2$ denotes distinct fluid regions.

The additional term $-\mu/k\vec{q}_i$ in the governing equation (7) is due to the porous medium (Chamkha [34]) where k is the permeability of the porous medium and $\vec{q}_i (i = 1, 2)$ is the velocity vector.

The current density $\vec{J}_i$ is expressed by Ohm's law (Gold [53]):

$$\vec{J}_i = \sigma_i \left(\vec{E} + \vec{q}_i \times \vec{B} \right), \tag{8}$$

where $\sigma_i (i = 1, 2)$ and $\vec{E}$ stand for electrical conductivity of the fluids for regions I and II and electric field, respectively.

Here, $\vec{E} = 0$ as there is no external electric field, and $|\vec{B}| = B_0$ because of our assumption that the induced magnetic field is too less (assumed to be zero) as compared to the external magnetic field. Hence, the Lorentz force is given by

$$\vec{F}_i = \vec{J}_i \times \vec{B} = \sigma_i \left(\vec{q}_i \times \vec{B} \right) \times \vec{B} = -\sigma_i B_0^2 \vec{q}_i. \tag{9}$$

Due to the unidirectional and symmetric nature of the flow, the fluid velocity vectors for both regions are to be in the form $\vec{q}_i = (0, 0, u_i(r))$ where $i = 1, 2$. These choices of velocities automatically satisfy the continuity equation (6) in respective flow regions. Under the above conditions, equation (7) governing the flow of the couple stress fluids in the respective regions can be written as follows:

In region I $(0 \le r \le R)$ (core region), we have

$$-\eta_1 \nabla^4 u_1 + \mu_1 \nabla^2 u_1 - \left(\frac{\mu_1}{k} + \sigma_1 B_0^2 \right) u_1 = \frac{\partial P}{\partial z}. \tag{10}$$

In region II $(R \le r \le R_0)$ (peripheral region), we have

$$-\eta_2 \nabla^4 u_2 + \mu_2 \nabla^2 u_2 - \left(\frac{\mu_2}{k} + \sigma_2 B_0^2 \right) u_2 = \frac{\partial P}{\partial z}, \tag{11}$$

where ∇^2 is the differential operator defined as

$$\nabla^2 = \frac{d^2}{dr^2} + \frac{1}{r} \frac{d}{dr}. \tag{12}$$

From equations (3) and (4), the force stress tensor τ_{ij} and couple stress tensor m_{ij} of the couple stress fluids are given by

$$\tau_{rz(i)} = \frac{d}{dr} \left[\mu_i u_i - \eta_i \nabla^2 u_i \right], i = 1, 2, \tag{13}$$

$$m_{r\theta(i)} = \eta_i \frac{d^2 u_i}{dr^2} - \frac{\eta_i{}'}{r} \frac{du_i}{dr}, i = 1, 2. \tag{14}$$

To determine $u_1(r)$ and $u_2(r)$, the boundary and interface conditions have to be specified.

3.1. Boundary and Interface Conditions. The description and mathematical form of the boundary conditions are presented in this section.

Instead of the usual no-slip condition, the slip velocity is taken on the surface of the rigid cylinder. In 1823, Navier [54] suggested a general boundary condition that presents the possibility of slipping at the solid boundary. This condition states that the tangential velocity of the fluid relative to the solid at a point on its surface is proportional to the tangential stress acting at that point. The proportionality that characterizes the surface's "slipperiness" is known as the slip length.

In view of the higher-order nature of governing equations, additional boundary conditions are required to find the solution. In addition to the Navier slip boundary condition, we use the Stokes (Stokes [5]) boundary conditions to solve the governing equations of the flow under consideration. The Stokes boundary condition assumes that the couple stresses vanish on the boundary of the solid.

The slip boundary condition along with zero couple stresses on the boundary is not sufficient to find the solution to the problem. A characteristic feature of the two-fluid flow problem is the coupling across the fluid/fluid interface. The fluid layers are mechanically coupled via the transfer of momentum across the interface. By the virtue of coupling of fluid layers at the fluid-fluid interface through momentum transfer, the continuity conditions for the velocity, vorticity, couple stress, and shear stress are adopted at the fluid-fluid interface. Therefore, the following physically realistic and mathematically consistent boundary and interface conditions are used for the considered physical model:

(i) The slip condition along with vanishing couple stresses are taken at the boundary of cylindrical pipe $r = R_0$

Following Punnamchandar and Fekadu [51], the slip condition gives

$$u_2(R_0) = \pm \gamma_s^{\star} \tau_{rz(2)}(R_0), \tag{15}$$

where $\gamma_s^{\star}$ such that $(0 \le \gamma_s^{\star} < \infty)$ corresponds to the slip coefficient at the upper boundary (Navier [54]). Note that as $\gamma_s^{\star} = 0$, the classical no-slip case is recovered (Devakar and Ramgopal [31]).

Following Srinivas and Murthy [32], the vanishing of couple stress on the surface of the cylinder leads to

$$m_{r\theta(2)}(R_0) = 0. \tag{16}$$

(ii) The continuity conditions for the velocity, vorticity, shear stress, and couple stress are adopted at the fluid-fluid interface. Following Kumar and Agrawal [44], this implies

$$u_1(r) = u_2(r) \text{ at } r = R, \tag{17}$$

$$\frac{du_1(r)}{dr} = \frac{du_2(r)}{dr} \text{ at } r = R, \tag{18}$$

$$\tau_{rz(1)}(r) = \tau_{rz(2)}(r) \text{ at } r = R, \tag{19}$$

$$m_{r\theta(1)}(r) = m_{r\theta(2)}(r) \text{ at } r = R. \tag{20}$$

(iii) Regularity condition: the axisymmetric flow suggested that the velocity of the fluid is finite on the axis of the cylinder $r = 0$. Following Devakar and Ramgopal [31], this implies

$$u_1(r) \text{ is finite at } r = 0. \tag{21}$$

To solve equation (10) and equation (11) under the boundary conditions (equation (15)–equation (21)), we make use of the following nondimensional quantities:

$$\begin{aligned} r^* &= \frac{r}{R}, \\ z^* &= \frac{z}{R}, \\ u_i^* &= \frac{u_i}{u_0}, \\ P^* &= \frac{P}{\rho_1 u_0^2}, \\ s &= \frac{R_0}{R}, \\ \gamma_s &= \frac{\gamma_s^* \mu_2}{R}, \end{aligned} \tag{22}$$

where u_0 and R are characteristic velocity and radius for the given flow model, respectively, and $i = 1, 2$ denotes distinct fluid regions.

Using the dimensionless variables in equations (10) and (11), the nondimensional form of the governing equations (after dropping the stars) is as follows:

For the core region I $(0 \le r \le 1)$, we have

$$\nabla^4 u_1 - s_1^2 \nabla^2 u_1 + s_1^2 \left(\frac{1}{Da} + M^2 \right) u_1 = s_1^2 ReG. \tag{23}$$

For the peripheral region II $(1 \le r \le s)$, we have

$$\nabla^4 u_2 - s_2^2 \nabla^2 u_2 + s_2^2 \left(\frac{1}{Da} + {M_1}^2 \right) u_2 = \frac{s_2^2 ReG}{n_\mu}, \tag{24}$$

where

$$\begin{aligned} s_i^2 &= \frac{\mu_i R^2}{\eta_i}, \\ M^2 &= \frac{B_0^2 R^2 \sigma_1}{\mu_1}, \\ M_1 &= M \sqrt{\frac{n_\sigma}{n_\mu}}, \\ n_\sigma &= \frac{\sigma_2}{\sigma_1}, \\ n_\mu &= \frac{\mu_2}{\mu_1}, \\ Da &= \frac{k}{R^2}. \end{aligned} \tag{25}$$

In the above equations, $G = -\partial P/\partial z$ is a constant pressure gradient, $\mathrm{Re} = \rho_1 UR/\mu_1$ is the Reynolds number, $s_i^2 = \mu_i R^2/\eta_i$ is the couple stress parameter, $Da = k/R^2$ is the Darcy number, $n_\sigma = \sigma_2/\sigma_1$ is the conductivity ratio, $M = B_0 R \sqrt{\sigma_1/\mu_1}$ is the magnetic number, and $n_\mu = \mu_2/\mu_1$ is the viscosity ratio.

From equations (13) and (44), the nondimensional forms of the shear stresses and couple stresses are

$$\tau_{rz(i)} = \frac{u_0 \mu_i}{R} \frac{d}{dr} \left[u_i - \frac{1}{s_i^2} \nabla^2 u_i \right], i = 1, 2, \tag{26}$$

$$m_{r\theta(i)} = \frac{u_0 \eta_i}{R^2} \left[\frac{d^2 u_i}{dr^2} - \frac{{\eta'}_i}{\eta_i} \frac{1}{r} \frac{du_i}{dr} \right], i = 1, 2. \tag{27}$$

4. Solution of the Problem

4.1. Flow Velocity in the Two Regions. The methodology used to get the general solution of the nondimensional differential equations (23) and (24) governing the fluids flow is as follows: finding the complementary solution $u_c(r)$ of the homogenous differential equation and then determining the particular solution $u_p(r)$ of the nonhomogeneous differential equation. Thus, the general solution can be constructed as

$$u_i(r) = u_c(r) + u_p(r). \tag{28}$$

Region I $(0 \le r \le 1)$:
Let

$$\alpha_1^2 + \alpha_2^2 = s_1^2, \tag{29}$$

$$\alpha_1^2\alpha_2^2 = s_1^2\left(\frac{1}{Da} + M^2\right). \tag{30}$$

Then, the equation (23) governing the fluid in region I can be written as

$$\left(\nabla^2 - \alpha_1^2\right)\left(\nabla^2 - \alpha_2^2\right)u_1 = ReGs_1^2, \tag{31}$$

where

$$\alpha_1^2, \alpha_2^2 = \frac{s_1^2 \pm \sqrt{s_1^4 - 4s_1^2((1/Da) + M^2)}}{2}. \tag{32}$$

First, we consider the corresponding homogeneous differential equation

$$\left(\nabla^2 - \alpha_1^2\right)\left(\nabla^2 - \alpha_2^2\right)u_1 = 0. \tag{33}$$

The solution of (33) is obtained by using the superposition principle such that

$$u_c^{(1)}(r) = y_1(r) + y_2(r), \tag{34}$$

where

$$\left(\nabla^2 - \alpha_1^2\right)y_1 = 0, \tag{35}$$

$$\left(\nabla^2 - \alpha_2^2\right)y_2 = 0. \tag{36}$$

Further, the differential equations (35) and (36) can be reduced to the following modified Bessel differential equations:

$$r^2\frac{d^2y_i}{dr^2} + \frac{1}{r}\frac{dy_i}{dr} - \alpha_i^2 r^2 y_i = 0, i = 1, 2. \tag{37}$$

The solutions to the above two equations (35) and (36), respectively, are

$$y_1(r) = C_1 I_0(\alpha_1 r) + C_2 K_0(\alpha_1 r), \tag{38}$$

$$y_2(r) = C_3 I_0(\alpha_2 r) + C_4 K_0(\alpha_2 r). \tag{39}$$

Inserting the expressions (38) and (39) into (34), we obtain the general solution of equation (33) as

$$u_c(r) = C_1 I_0(\alpha_1 r) + C_2 K_0(\alpha_1 r) + C_3 I_0(\alpha_2 r) + C_4 K_0(\alpha_2 r). \tag{40}$$

The particular solution of the differential equation (31) can be easily obtained as

$$y_p(r) = \frac{ReGs_1^2}{\alpha_1^2\alpha_2^2}. \tag{41}$$

Therefore, the general solution of the differential equation (31), after substituting (40) and (41) in equation (28), becomes

$$\begin{aligned} u_1(r) = {} & C_1 I_0(\alpha_1 r) + C_2 K_0(\alpha_1 r) + C_3 I_0(\alpha_2 r) \\ & + C_4 K_0(\alpha_2 r) + \frac{ReGs_1^2}{\alpha_1^2\alpha_2^2}, \end{aligned} \tag{42}$$

where C_1, C_2, C_3, and C_4 are arbitrary constants.

Region-II ($1 \le r \le s$):

Let

$$\beta_1^2 + \beta_2^2 = s_2^2, \tag{43}$$

$$\beta_1^2\beta_2^2 = s_2^2\left(\frac{1}{Da} + {M_1}^2\right). \tag{44}$$

Then, equation (24) governing fluid flow in region II can be written as

$$\left(\nabla^2 - \beta_1^2\right)\left(\nabla^2 - \beta_2^2\right)u_2 = \frac{\mathrm{Re}\ Gs_2^2}{n_\mu}, \tag{45}$$

where for region II,

$$\beta_1^2, \beta_2^2 = \frac{s_2^2 \pm \sqrt{s_2^4 - 4s_2^2((1/Da) + {M_1}^2)}}{2}. \tag{46}$$

Therefore, similarly solving equation (45) by the method stated above, we get

$$\begin{aligned} u_2(r) = {} & D_1 I_0(\beta_1 r) + D_2 K_0(\beta_1 r) + D_3 I_0(\beta_2 r) \\ & + D_4 K_0(\beta_2 r) + \frac{ReGs_2^2}{n_\mu \beta_1^2\beta_2^2}, \end{aligned} \tag{47}$$

where D_1, D_2, D_3, and D_4 are arbitrary constants.

The closed-form solutions of the differential equations (31) and (45) are given by equations (42) and (47) contain modified Bessel functions. Here, $I_0(\alpha_1 r)$, $I_0(\alpha_2 r)$, $I_0(\beta_1 r)$, and $I_0(\beta_2 r)$ and $K_0(\alpha_1 r)$, $K_0(\alpha_2 r)$, $K_0(\beta_1 r)$, and $K_0(\beta_2 r)$ are the first kind modified Bessel's functions of zero order and the second kind modified Bessel's functions of zero order, respectively.

4.2. Stress in the Two Regions. From equation (26), the nondimensional tangential stress of the fluid in region I is given by

$$\begin{aligned} \tau_{rz(1)} = \frac{\mu_1 u_0}{R}\Bigg[& \left(\alpha_1 - \frac{\alpha_1^3}{s_1^2}\right)(I_1(r\alpha_1)C_1 - K_1(r\alpha_1)C_2) \\ & + \left(\alpha_2 - \frac{\alpha_2^3}{s_1^2}\right)(I_1(r\alpha_2)C_3 - K_1(r\alpha_2)C_4)\Bigg]. \end{aligned} \tag{48}$$

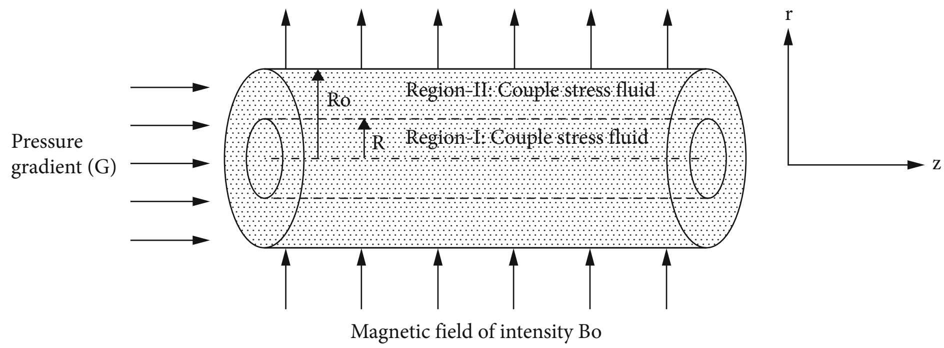

Figure 1: Geometrical configuration.

From equation (27), the couple stress in region I is given by

$$m_{r\theta(1)} = \frac{\eta_1 u_0}{R^2}\left[\left(\alpha_1^2 I_0(r\alpha_1) - \frac{\alpha_1}{r}\left(1+\frac{\eta_1'}{\eta_1}\right)I_1(r\alpha_1)\right)C_1 + \left(\alpha_1^2 K_0(r\alpha_1) + \frac{\alpha_1}{r}\left(1+\frac{\eta_1'}{\eta_1}\right)K_1(r\alpha_1)\right)C_2 + \left(\alpha_2^2 I_0(r\alpha_2) - \frac{\alpha_2}{r}\left(1+\frac{\eta_1'}{\eta_1}\right)I_1(r\alpha_2)\right)C_3 + \left(\alpha_2^2 K_0(r\alpha_2) + \frac{\alpha_2}{r}\left(1+\frac{\eta_1'}{\eta_1}\right)K_1(r\alpha_2)\right)C_4\right]. \quad (49)$$

Similarly, tangential stress in region II given by equation (26) becomes

$$\tau_{rz(2)} = \frac{\mu_2 u_0}{R}\left[\left(\beta_1 - \frac{\beta_1^3}{s_2^2}\right)(I_1(r\alpha_1)D_1 - K_1(r\beta_1)D_2) + \left(\beta_2 - \frac{\beta_2^3}{s_2^2}\right)(I_1(r\beta_2)D_3 - K_1(r\beta_2)D_4)\right]. \quad (50)$$

The couple stress of fluid in region II given by equation (26) becomes

$$m_{r\theta(2)} = \frac{\eta_2 u_0}{R^2}\left[\left(\beta_1^2 I_0(r\beta_1) - \frac{\beta_1}{r}\left(1+\frac{\eta_2'}{\eta_2}\right)I_1(r\beta_1)\right)D_1 + \left(\beta_1^2 K_0(r\beta_1) + \frac{\beta_1}{r}\left(1+\frac{\eta_2'}{\eta_2}\right)K_1(r\beta_1)\right)D_2 + \left(\beta_2^2 I_0(r\beta_2) - \frac{\beta_2}{r}\left(1+\frac{\eta_2'}{\eta_2}\right)I_1(r\beta_2)\right)D_3 + \left(\beta_2^2 K_0(r\beta_2) + \frac{\beta_2}{r}\left(1+\frac{\eta_2'}{\eta_2}\right)K_1(r\beta_2)\right)D_4\right]. \quad (51)$$

To obtain a complete solution to the concerned problem, we have to determine the constants C_i and D_i for $i = 1, 2, 3, 4$. C_i and D_i for $i = 1, 2, 3, 4$ are calculated numerically by solving the algebraic system obtained from the boundary conditions.

4.3. Determination of Arbitrary Constants. Nondimensionalizing the boundary conditions (15)–(21), we have the following:

(i) Since the modified Bessel function of the second kind, i.e., $K_n(r)$, is not finite at a singular point $r = 0$, therefore for finite values of $u_1(r)$ along the axis of a cylindrical pipe, the coefficient of $K_n(\alpha_i r)$ for $n = 0, 1$ and $i = 1, 2$ should be zero. Thus, we have

$$C_2 = C_4 = 0. \quad (52)$$

(ii) The slip and vanishing of couple stress boundary conditions at $r = s$ give

$$u_2(s) = \pm\gamma_s \tau_{rz(2)}(s), \quad (53)$$

$$m_{r\theta(2)}(s) = 0, \quad (54)$$

where $\gamma_s = \gamma_s^\star \mu_2/R$ is the nondimensional slip parameter

(iii) Continuity of velocities, vorticites, shear stresses and couple stresses at the fluid-fluid interface $r = 1$ are as follows:

$$u_1(r) = u_2(r), \quad (55)$$

$$\frac{du_1(r)}{dr} = \frac{du_2(r)}{dr}, \quad (56)$$

$$\tau_{rz(1)}(1) = \tau_{rz(2)}(1), \quad (57)$$

$$m_{r\theta(1)}(1) = m_{r\theta(2)}(1). \quad (58)$$

Substituting equation (42) and equations (47)–(51) in equations (52)–(58), the linear system of an algebraic equation with six unknown arbitrary constants C_1, C_3, and D_i for $i = 1, 2, 3, 4$ involved in the solution of the problem is

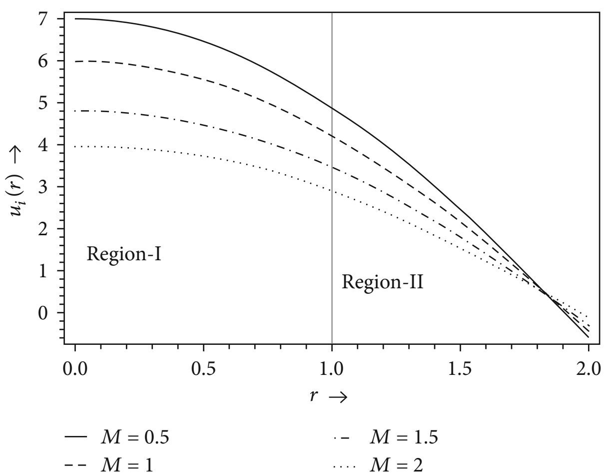

Figure 2: Variations of $u_i(r)(i = 1, 2)$ against M when $Da = 1.0$, $\mathrm{Re} = 2$, $n_\sigma = 1.0$, $n_\mu = 1.1$, $\gamma_s = 0.1$, $G = 10$, $s_1 = 1$, $s_2 = 1$, and $s = 2$.

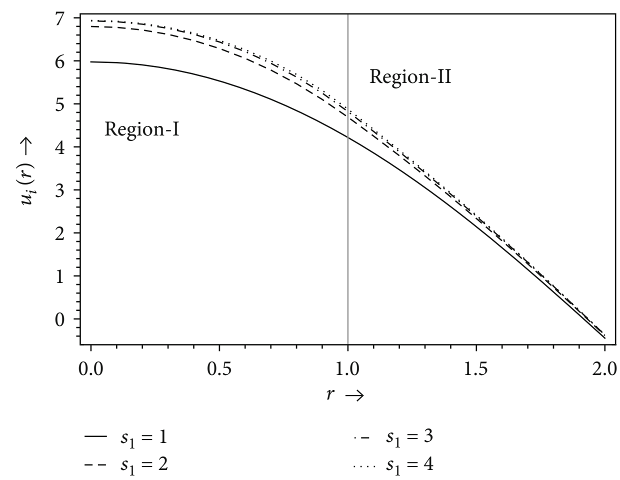

Figure 3: Variations of $u_i(r)(i = 1, 2)$ with s_1 when $Da = 1.0$, $M = 1$, $\mathrm{Re} = 2$, $n_\sigma = 1.0$, $n_\mu = 1.1$, $\gamma_s = 0.1$, $G = 10$, $s_2 = 1$, and $s = 2$.

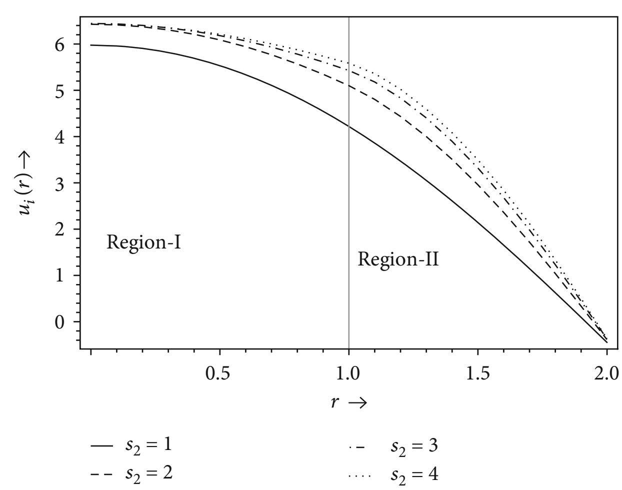

Figure 4: Variations of $u_i(r)(i = 1, 2)$ with s_2 when $Da = 1.0$, $M = 1$, $\mathrm{Re} = 2$, $n_\sigma = 1.0$, $n_\mu = 1.1$, $\gamma_s = 0.1$, $G = 10$, $s_1 = 1$, and $s = 2$.

formed. Using Mathematica software, all constants C_1, C_3, and D_i for $i = 1, 2, 3, 4$ have been evaluated uniquely using the above boundary conditions. Owing to the lengthy expressions of these constants, they are not presented here.

4.4. Total Flow Rate. The nondimensional volumetric flow rate across the whole cross-section of a porous cylinder is given by (Devakar and Ramgopal [31])

$$Q = \int_0^{2\pi} \left[\int_0^1 r u_1 dr + \int_1^2 r u_2 dr \right] d\theta. \tag{59}$$

Invoking the values of $u_1(r)$ and $u_2(r)$ from equations (42) and (47) in equation (59) and integrating, we obtain

$$\begin{aligned} Q = 2\pi \Bigg[& C_1 \frac{I_1(\alpha_1)}{\alpha_1} + C_3 \frac{I_1(\alpha_2)}{\alpha_2} + \frac{ReDaG}{2\left(1 + DaM^2\right)} \\ & \cdot (sI_1(s\beta_1) - I_1(s\beta_1)) \frac{D_1}{\beta_1} - (sK_1(s\beta_1) - K_1(s\beta_1)) \frac{D_2}{\beta_1} \\ & + (sI_1(s\beta_2) - I_1(s\beta_2)) \frac{D_3}{\beta_2} - (sK_1(s\beta_2) - K_1(s\beta_2)) \frac{D_4}{\beta_2} \\ & + \frac{ReGDa\left(s^2 - 1\right)}{2n_\mu\left(1 + DaM_1^2\right)} \Bigg]. \end{aligned} \tag{60}$$

5. Results and Discussion

Analytical solutions for the steady, laminar hydromagnetic flow of two immiscible and incompressible couple stress fluids through porous medium in a horizontal cylinder have been obtained. The numerical evaluation of the analytical expressions for velocity profile and flow rate are done for different flow parameters values, such as the magnetic number, couple stress parameter, Reynolds number, Darcy number, ratio of viscosities, slip parameter, and pressure gradient using Mathematica software package. The numerical values for each case, when a particular parameter is varied, are obtained by keeping $Da = 1.0$, $M = 1$, $\mathrm{Re} = 2$, $n_\sigma = 1.0$, $n_\mu = 1.1$, $\gamma_s = 0.1$, $G = 10$, $s_1 = 1$, $s_2 = 1$, and $s = 2$.

The variations of velocity profiles for different flow parameters are shown graphically through Figures 2–9. Figure 2 illustrates the influence of the magnetic number M on the velocities. It is observed that the fluid velocities in both regions are decreasing with an increment of magnetic number M. This finding suggests that the magnetic field applied to the flow system retards the motion of the fluid. This is consistent with the fact that a strong magnetic field applied to the flow literally increases the Lorentz force, which strongly opposes the fluid's motion and lowers the velocities. This result is validated by the works of Ansari and Deo [41], Kumar and Agarwal [44], and Punnamchandar and Fekadu [51, 52]. Further, as $M \longrightarrow 0$, the magnetic number loses its properties and behaves as a normal flow in the absence of a magnetic field (Srinivas and Murthy [32]).

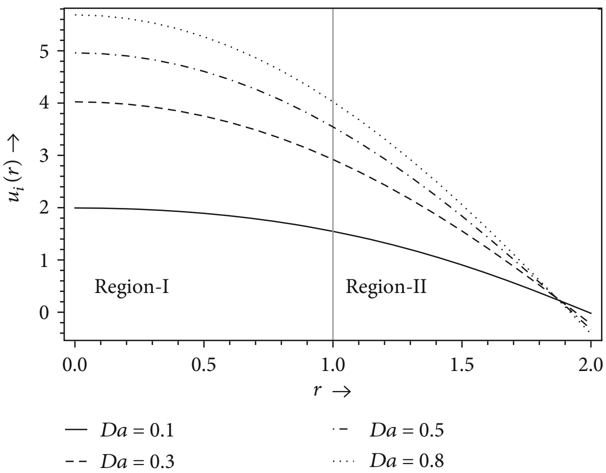

FIGURE 5: Variations of $u_i(r)(i = 1, 2)$ with Da when $M = 1$, $\mathrm{Re} = 2$, $n_\sigma = 1.0$, $n_\mu = 1.1$, $\gamma_s = 0.1$, $G = 10$, $s_1 = 1$, $s_2 = 1$, and $s = 2$.

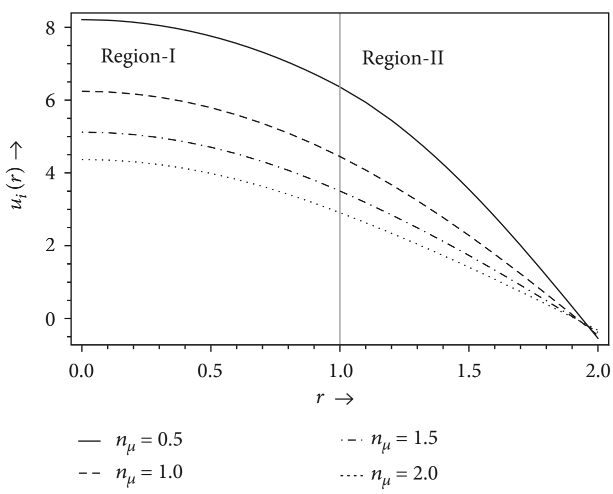

FIGURE 6: Variations of $u_i(r)(i = 1, 2)$ with n_μ when $Da = 1.0$, $M = 1$, $\mathrm{Re} = 2$, $n_\sigma = 1.0$, $\gamma_s = 0.1$, $G = 10$, $s_1 = 1$, $s_2 = 1$, and $s = 2$.

The effects of couple stress parameters s_1 and s_2 on the flow are displayed in Figures 3–4. The effect of the couple stress parameter s_1 on the flow velocity profiles is seen in Figure 3. In this case, we notice that a rise in the couple stress parameter s_1 causes the fluid's velocity to increase in both flow areas. Figure 4 shows a similar trend when varied with the couple stress parameter s_2. Therefore, we draw the conclusion that raising couple stress parameters s_i for $i = 1, 2$ causes fluid velocities to increase in both flow areas. This result validates our problem with the previous works of Umavathi et al. [20], Devakar et al. [23], Srinivas and Murthy [32], Srinivas et al. [37], and Kumar and Agarwal [44]. Since $s_i^2 = \mu_i R^2/\eta_i$, an increase in couple stress viscosities η_i for $i = 1, 2$ corresponds to a decrease in the couple stress parameters s_i. As a result, increasing couple stress coefficients η_i for $i = 1, 2$ has a retarding effect on fluid velocities. This indicates that the presence of couple stress in the fluid reduces the velocity of a fluid. This is due to the fact that physically, the couple stresses expend some energy to rotate the particles, which reduces the particles' velocity.

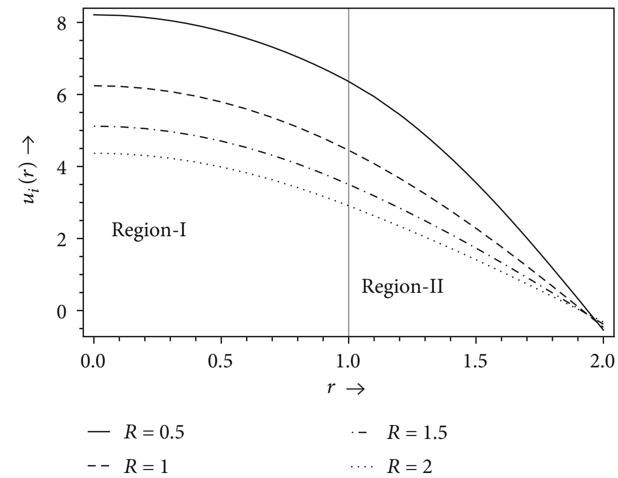

FIGURE 7: Variations of $u_i(r)(i = 1, 2)$ with Re when $Da = 1.0$, $M = 1$, $n_\sigma = 1.0$, $n_\mu = 1.1$, $\gamma_s = 0.1$, $G = 10$, $s_1 = s_2 = 1$, and $s = 2$.

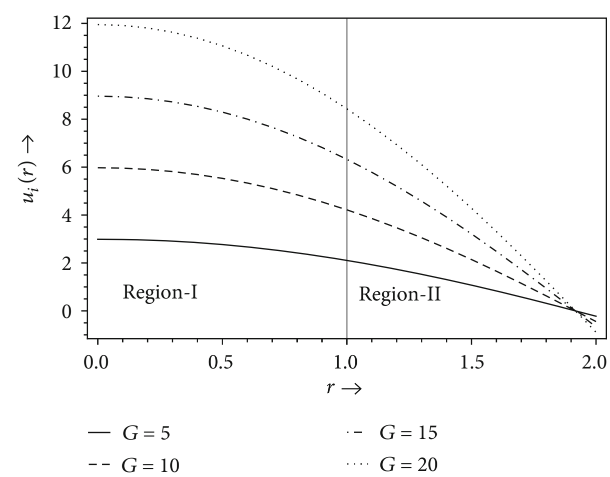

FIGURE 8: Variations of $u_i(r)(i = 1, 2)$ with G when $Da = 1.0$, $M = 1$, $\mathrm{Re} = 2$, $n_\sigma = 1.0$, $n_\mu = 1.1$, $\gamma_s = 0.1$, $s_1 = 1$, $s_2 = 1$, and $s = 2$.

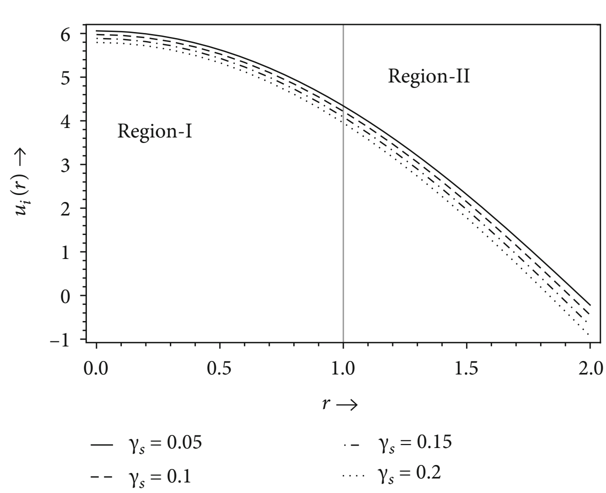

FIGURE 9: Variations of $u_i(r)(i = 1, 2)$ with γ_s when $Da = 1.0$, $M = 1$, $\mathrm{Re} = 2$, $n_\sigma = 1.0$, $n_\mu = 1.1$, $G = 10$, $s_1 = 1$, $s_2 = 1$, and $s = 2$.

Table 1: Variations of $Q_i (i = 1, 2)$ and Q with respect to M.

M	Q1	Q2	Q
0.	19.6805	20.0851	39.7655
1	15.9975	16.9066	32.904
1.5	12.9213	14.2132	27.1345
2.	10.8443	12.4318	23.2761

Table 2: Variations of $Q_i (i = 1, 2)$, Q with respect to s_1.

s_1	Q1	Q2	Q
1	15.9975	16.9066	32.904
2	18.0884	18.7352	36.8237
3	18.5571	19.2242	37.7813
4	18.7069	19.4358	38.1428

Table 3: Variations of $Q_i (i = 1, 2)$, Q with respect to s_2.

s_2	Q1	Q2	Q
1	15.9975	16.9066	32.904
2	18.0883	23.0374	41.1257
3	18.6223	25.6862	44.3085
4	18.8456	26.9956	45.8412

Table 4: Variations of $Q_i (i = 1, 2)$, Q with respect to Da.

Da	Q1	Q2	Q
0.1	5.58574	7.23685	12.8226
0.3	10.9187	12.3188	23.2375
0.5	13.3591	14.5399	27.899
0.8	15.2487	16.2378	31.4865

Table 5: Variations of $Q_i (i = 1, 2)$, Q with respect to n_μ.

n_μ	Q1	Q2	Q
0.5	22.9166	27.7223	50.6389
1.	16.7912	17.9853	34.7765
1.5	13.5173	13.7398	27.2571
2.	11.3849	11.2239	22.6088

Table 6: Variations of $Q_i (i = 1, 2)$, Q with respect to Re.

Re	Q1	Q2	Q
1	16.7912	17.9853	34.7765
2	11.3849	11.2239	22.6088
3	8.71848	8.28735	17.0058
4	7.09974	6.59498	13.6947

Furthermore, it is to be noted that in the absence of couple stresses, that is, as $\eta_i \longrightarrow 0$, the parameter $s_i \longrightarrow \infty$, the properties of couple stress in the fluid vanish and the case of classical viscous fluid can be obtained from this work (Umavathi et al. ([28–30]), Abbas et al. [22], Devakar et al. [23], and Devakar and Ramgopal [31]). Therefore, it is understood that the velocity in the case of couple stress fluid is lower than that of a Newtonian fluid.

The effect of Darcy's number Da on the fluid velocities is shown in Figure 5. From this figure, it is noticed that the velocities in both fluid regions increase with the increase of Darcy's number Da. Since $Da = k/R^2$, an increase in Darcy's number corresponds to an increase in the permeability (permeable parameter k) of the porous medium, which supports the flow. Lesser permeability causes a slighter fluid velocity to be observed inside the flow medium occupied by the fluid. Thus, it may be concluded that an increase in the Darcy's number enhances fluid velocities. This is due to the reason that the additional flow resistance that the porous structure offers diminishes as Da (permeable parameter k) gradually increases. A similar kind of behavior can be found in Refs. Srinivas and Murthy [32], Srinivas et al. [37], Punnamchandar and Fekadu [51], and Kumar and Agarwal [44].

Figure 6 describes the effect of the ratio of viscosities n_μ on velocity profiles. Figure 6 reveals that as the viscosity ratio n_μ increases, the velocity of the fluid decreases in both flow regions. This is because as the viscosity ratio n_μ increases, greater flow resistance is provided. As a result, velocity drops. Therefore, we conclude that an increase in the ratio of viscosities inhibits fluid motion. A similar view can be found in the works of Umavathi et al. [21], Umavathi et al. [30], Srinivas and Murthy [32], and Punnamchandar and Fekadu [51]. Figure 7 presents the effect of the Reynolds number on the velocity profile. Thereby, we observe that as the Reynolds number Re increases, there is a decrease in the velocities of the fluid in both flow regions. This indicates that velocity is reduced by the increase of the Reynolds number Re and our results well agreed with the results of Devakar et al. [23], Devakar and Ramgopal [31], Srinivas and Murthy [32], and Punnamchandar and Fekadu [51].

Figure 8 represents the velocity profile for the different values of the pressure gradient. It is observed that with the increase in G, velocity is increasing in both the fluid regions. Physically, the more the pressure gradient, the more the fluid is pushed to generate the flow, which results in an increase in fluid velocity. Figure 9 displays the effect of the slip parameter γ_s on the fluid flow velocity profiles. Figure 9 shows that increasing the slip parameter reduces fluid velocity in both zones. Obviously, fluid slippage has the opposite impact on fluid motion, and increasing the slip parameter reduces the velocity significantly in both regions. A similar trend was observed in the work of Punnamchandar and Fekadu [51, 52]. Furthermore, when the slip parameter is set to zero, the classical case of no slip is recovered as a special case.

The numerical values of the volume flow rate are computed for various pertinent flow parameters and are presented in Tables 1–8. The effect of the magnetic number M on the flow rate is shown in Table 1. From Table 1, we notice that the total flow rate decreases as the magnetic number M increases from 0.5 to 2 for fixed values of $Da = 1.0$, $\mathrm{Re} = 2$, $n_\sigma = 1.0$, $n_\mu = 1.1$, $\gamma_s = 0.1$, $G = 10$, $s_1 = 1$, $s_2 = 1$, and $s = 2$. Tables 2 and 3 shows the nature of flow rates for different values of couple stress parameter s_i, $i = 1, 2$. From the tables, we can see that the total flow rate increases with an increase

Table 7: Variations of $Q_i (i = 1, 2)$, Q with respect to G.

G	Q1	Q2	Q
5	7.99873	8.45329	16.452
10	15.9975	16.9066	32.904
15	23.9962	25.3599	49.3561
20	31.9949	33.8132	65.8081

Table 8: Variations of $Q_i (i = 1, 2)$, Q with respect to γ_s.

γ_s	Q1	Q2	Q
0.05	16.3244	18.5806	34.905
0.1	15.9975	16.9066	32.904
0.15	15.656	15.1585	30.8145
0.2	15.2991	13.3312	28.6303

of couple stress parameters s_i, $i = 1, 2$. Table 4 demonstrates the effect of Darcy's number on the flow rate. From Table 4, we can see that the total flow rate increases with an increase in Darcy's number. Table 5 shows the effect of the viscosity ratio on the flow rate. The flow rate shows a decreasing trend with the growth of the viscosity ratio. Table 6 displays various values of flow rate with respect to the Reynolds number. It is seen from Table 6 that as the Reynolds number increases, the total flow rate decreases. Table 7 represents the flow rate for the different pressure gradient values. From the table, it is observed that increasing the pressure gradient increases the volume flow rate across the pipe cross-section. Table 8 presents the numerical flow rate data with respect to slip parameter γ_s. It is observed that the volume flow rate gets decreased with an increase of slip parameter γ_s.

6. Conclusions

The problem of steady, laminar, and fully developed hydromagnetic flow of two immiscible couple stress fluids through a porous medium in a horizontal cylinder under the effect of the Navier slip boundary condition is considered in the present study. The motion is generated by a constant pressure gradient delivered along the axial direction, i.e., z-axis. The resulting set of coupled differential equations associated with the flow of the two fluids subject to the appropriate boundary and interface conditions is solved analytically. Exact solutions are obtained in terms of the modified Bessel functions. The effects of various physical parameters on the velocity profiles and total flow rate are studied. The significant findings of the current investigation are the following:

(i) Increasing the magnetic number, viscosity ratio, Reynolds number, and slip parameter reduces fluid velocities

(ii) The increment of the couple stress parameters, Darcy number, and pressure gradient enhances the fluid velocity in both flow regions

(iii) Increase in the magnetic number, slip parameter, viscosity ratio, and Reynolds number suppress the volume flow rate

(iv) Increase in the couple stress parameter, Darcy number, and pressure gradient promotes volume flow rate

This work can be extended to the unsteady flow problem and is also made to include heat transfer/thermal effects. We would like extend this work by taking various fluids like micropolar fluid, or any other non-Newtonian fluid.

Nomenclature

B_0:	Magnetic field intensity
$C_i, D_i, (i = 1, 2, 3, 4)$:	Arbitrary constants
Da:	Darcy number
G:	Pressure gradient
$\vec{J}$:	Current density
M:	Magnetic number
m_{ij}:	Couple stress
P:	Fluid pressure at any point
$\vec{q}_i (i = 1, 2)$:	Velocity vector in regions I and II
Q:	Total volumetric flow rate
$Q_i (i = 1, 2)$:	Flow rate in regions I and II
R:	Radius of the inner cylindrical region
Re:	Reynolds number
R_0:	Radius of the cylinder
s:	$= R_0/R$, radius ratio
$s_i (i = 1, 2)$:	Couple stress parameters
$u_i (i = 1, 2)$:	Velocity components
∇^2:	The operator $d^2/dr^2 + (1/r)(d/dr)$
r, θ, z:	Cylindrical coordinates
$I_n(.), K_n(.)$:	Modified Bessel functions
η_i, η'_i:	Couple stress viscosity coefficients
γ_s:	Nondimensional slip parameter
γ_s^*:	Slip coefficient
$\mu_i (i = 1, 2)$:	Dynamic viscosity coefficients
n_μ:	Ratio of viscosities
$\rho_i (i = 1, 2)$:	Density of fluid in regions I and II
$\sigma_i (i = 1, 2)$:	Electrical conductivity
n_σ:	Ratio of electrical conductivity
τ_{ij}:	Shear stress.

Data Availability

No data were used to support this study.

Conflicts of Interest

The authors declare that they have no conflicts of interest.

References

[1] A. C. Eringen, "Simple microfluids," *International Journal of Engineering Science*, vol. 2, no. 2, pp. 205–217, 1964.

[2] T. T. Ariman and N. D. Sylvester, "Microcontinuum fluid mechanics–a review," *International Journal of Engineering Science*, vol. 11, no. 8, pp. 905–930, 1973.

[3] S. C. Cowin, "The theory of polar fluids," in *Advances in Applied Mechanics*, vol. 14, pp. 279–347, Academic Press, New York, 1974.

[4] V. K. Stokes, "Couple stresses in fluids," *Physics of Fluids*, vol. 9, no. 9, pp. 1709–1715, 1966.

[5] V. K. Stokes, *Theories of Fluids with Microstructure*, Springer-Verlag, Berlin, 1984.

[6] L. M. Srivastava, "Peristaltic transport of a couple-stress fluid," *Rheologica Acta*, vol. 25, no. 6, pp. 638–641, 1986.

[7] E. F. E. I. Shehawey and K. H. S. Mekheimer, "Couple-stresses in peristaltic transport of fluids," *Journal of Physics D: Applied Physics*, vol. 27, no. 6, pp. 1163–1170, 1994.

[8] J. Lin, "Squeeze film characteristics of finite journal bearings: couple stress fluid model," *Tribology International*, vol. 31, no. 4, pp. 201–207, 1998.

[9] E. Walicki and A. Walicka, "Inertial effect in the squeeze film of couple-stress fluids in biological bearings," *International Journal of Applied Mechanics and Engineering*, vol. 4, pp. 363–373, 1999.

[10] X. Wang, K. Zhu, and C. Gui, "A study of a journal bearing lubricated by couple stress fluids considering thermal and cavitation effects," *Proceedings of the Institution of Mechanical Engineers, Part J: Journal of Engineering Tribology*, vol. 216, no. 5, pp. 293–305, 2002.

[11] N. B. Naduvinamani, T. F. Syeda, and P. S. Hiremath, "Hydrodynamic lubrication of rough slider bearings with couple stress fluids," *Tribology International*, vol. 36, no. 12, pp. 949–959, 2003.

[12] D. Pal, N. Rudraiah, and R. Devanathan, "A couple stress model of blood flow in the microcirculation," *Bulletin of Mathematical Biology*, vol. 50, no. 4, pp. 329–344, 1988.

[13] M. Sahu, S. Sharma, and A. Agrawal, "Study of arterial blood flow in stenosed vessel using non-newtonian couple stress fluid model," *International Journal of Dynamics of Fluids*, vol. 6, no. 2, pp. 248–257, 2000.

[14] D. Srinivasacharya and G. M. Rao, "Mathematical model for blood flow through a bifurcated artery using couple stress fluid," *Mathematical Biosciences*, vol. 278, pp. 37–47, 2016.

[15] P. Chaturani and R. P. Samy, "A study of non-Newtonian aspects of blood flow through stenosed arteries and its applications in arterial diseases," *Biorheology*, vol. 22, no. 6, pp. 521–531, 1985.

[16] P. Sinha and C. Singh, "Effects of couple stresses on the blood flow through an artery with mild stenosis," *Biorheology*, vol. 21, no. 3, pp. 303–315, 1984.

[17] K. C. Valanis and C. T. Sun, "Poiseuille flow of a fluid with couple stress with applications to blood flow," *Biorheology*, vol. 6, no. 2, pp. 85–97, 1969.

[18] M. Sharan and A. S. Popel, "A two-phase model for flow of blood in narrow tubes with increased effective viscosity near the wall," *Biorheology*, vol. 38, no. 5-6, pp. 415–428, 2001.

[19] A. E. Garcia and D. N. Riahi, "Two-phase blood flow and heat transfer in an inclined stenosed artery with or without a catheter," *International Journal of Fluid Mechanics Research*, vol. 41, no. 1, pp. 16–30, 2014.

[20] J. C. Umavathi, A. J. Chamkha, M. H. Manjula, and A. Al-Mudhaf, "Flow and heat transfer of a couple stress fluid sandwiched between viscous fluid layers," *Canadian Journal of Physics*, vol. 83, no. 7, pp. 705–720, 2005.

[21] J. C. Umavathi, M. H. Manjula, I. C. Liu, and I. Pop, "Flow and heat transfer of couple stress and viscous fluids in a vertical channel," *International Journal of Applied Mechanics and Engineering*, vol. 12, pp. 537–555, 2007.

[22] Z. Abbas, J. Hasnaina, and M. Sajid, "Hydromagnetic mixed convective two-phase flow of couple stress and viscous fluids in an inclined channel," *Zeitschrift für Naturforschung A*, vol. 69, no. 10-11, pp. 553–561, 2014.

[23] M. Devakar, A. Raje, and S. Hande, "Unsteady flow of couple stress fluid sandwiched between Newtonian fluids through a channel," *Zeitschrift für Naturforschung A*, vol. 73, no. 7, pp. 629–637, 2018.

[24] B. A. Packham and R. Shall, "Stratified laminar flow of two immiscible fluids," *Proceedings of the Cambridge Philosophical Society*, vol. 69, no. 3, pp. 443–448, 1971.

[25] A. R. Rao and S. Usha, "Peristaltic transport of two immiscible viscous fluids in a circular tube," *Journal of Fluid Mechanics*, vol. 298, pp. 271–285, 1995.

[26] A. J. Chamkha, J. C. Umavathi, and A. Mateen, "Oscillatory flow and heat transfer in two immiscible fluids," *International Journal of Fluid Mechanics Research*, vol. 31, no. 1, pp. 13–36, 2004.

[27] J. C. Umavathi, A. J. Chamkha, A. Mateen, and A. Al-Mudhaf, "Unsteady two-fluid flow and heat transfer in a horizontal channel," *Heat and Mass Transfer*, vol. 42, no. 2, pp. 81–90, 2005.

[28] J. C. Umavathi, I. C. Liu, and M. Shekar, "Unsteady mixed convective heat transfer of two immiscible fluids confined between long vertical wavy wall and parallel flat wall," *Applied Mathematics and Mechanics*, vol. 33, no. 7, pp. 931–950, 2012.

[29] J. C. Umavathi and M. Shekar, "Mixed convective flow of immiscible fluids in a vertical corrugated channel with traveling thermal waves," *Journal of King Saud University-Engineering Sciences*, vol. 26, no. 1, pp. 49–68, 2014.

[30] J. C. Umavathi, J. P. Kumar, and A. J. Chamkha, "Convective flow of two immiscible viscous and couple stress permeable fluids through a vertical channel," *Turkish Journal of Engineering and Environmental Sciences*, vol. 33, pp. 221–243, 2009.

[31] M. Devakar and N. C. Ramgopal, "Fully developed flows of two immiscible couple stress and Newtonian fluids through nonporous and porous medium in a horizontal cylinder," *Journal of Porous Media*, vol. 18, no. 5, pp. 549–558, 2015.

[32] J. Srinivas and J. V. R. Murthy, "Flow of two immiscible couple stress fluids between two permeable beds," *Journal of Applied Fluid Mechanics*, vol. 9, no. 1, pp. 501–507, 2016.

[33] P. K. Yadav, S. Jaiswal, J. Y. Puchakatla, and A. N. Filippov, "Poiseuille flow of micropolar-Newtonian fluid through concentric pipes filled with porous medium," *Colloid Journal*, vol. 82, no. 3, pp. 333–341, 2020.

[34] A. J. Chamkha, "Flow of two-immiscible fluids in porous and nonporous channels," *Journal of Fluids Engineering*, vol. 122, no. 1, pp. 117–124, 2000.

[35] S. T. Harmindar and A. K. Singh, "Free convection flow of two immiscible viscous liquids through parallel permeable beds: use of Brinkman equation," *International Journal of Fluid Mechanics Research*, vol. 32, no. 1, pp. 39–56, 2005.

[36] A. K. Singh, "Convective flow of two immiscible viscous fluids using Brinkmann model," *Indian Journal of Pure and Applied Physics*, vol. 43, pp. 415–442, 2005.

[37] J. Srinivas, J. V. Ramana Murthy, and K. S. Sai, "Entropy generation analysis of the flow of two immiscible couple stress fluids between two porous beds," *Computational Thermal Sciences*, vol. 7, no. 2, pp. 123–137, 2015.

[38] K. Vajravelu, P. V. Arunachalam, and S. Sreenadh, "Unsteady flow of two immiscible conducting fluids between two permeable beds," *Journal of Mathematical Analysis and Applications*, vol. 196, no. 3, pp. 1105–1116, 1995.

[39] M. S. Malashetty, J. C. Umavathi, and J. Prathap Kumar, "Two fluid flow and heat transfer in an inclined channel containing porous and fluid layer," *Heat and Mass Transfer*, vol. 40, no. 11, pp. 871–876, 2004.

[40] T. L. Raju and M. Nagavalli, "Unsteady two-layered fluid flow and heat transfer of conducting fluids in a channel between parallel porous plates under transverse magnetic field," *International Journal of Applied Mechanics and Engineering*, vol. 18, no. 3, pp. 699–726, 2013.

[41] I. A. Ansari and S. Deo, "Effect of magnetic field on the two immiscible viscous fluids flow in a channel filled with porous medium," *National Academy Science Letters*, vol. 40, no. 3, pp. 211–214, 2017.

[42] P. K. Yadav and S. Jaiswal, "Influence of an inclined magnetic field on the Poiseuille flow of immiscible micropolar-Newtonian fluids in a porous medium," *Canadian Journal of Physics*, vol. 96, no. 9, pp. 1016–1028, 2018.

[43] S. Jaiswal and P. K. Yadav, "Influence of magnetic field on the Poiseuille flow of immiscible Newtonian fluids through highly porous medium," *Journal of the Brazilian Society of Mechanical Sciences and Engineering*, vol. 42, no. 4, pp. 1–15, 2020.

[44] D. Kumar and M. Agarwal, "MHD pulsatile flow and heat transfer of two immiscible couple stress fluids between permeable beds," *Kyungpook Mathematical Journal*, vol. 61, pp. 323–351, 2021.

[45] A. B. Basset, *A Treatise on Hydrodynamics*, vol. 2, Dover, New York, NY, USA, 1961.

[46] B. S. Bhatt and N. C. Sacheti, "On the analogy in slip flows," *Indian Journal of Pure and Applied Mathematics*, vol. 10, pp. 303–306, 1979.

[47] P. A. Thompson and S. M. Troian, "A general boundary condition for liquid flow at solid surfaces," *Nature*, vol. 389, no. 6649, pp. 360–362, 1997.

[48] R. Ellahi, "Effects of the slip boundary condition on non-Newtonian flows in a channel," *Communications in Nonlinear Science and Numerical Simulation*, vol. 14, no. 4, pp. 1377–1384, 2009.

[49] M. Devakar, D. Sreenivasu, and B. Shankar, "Analytical solutions of couple stress fluid flows with slip boundary conditions," *Alexandria Engineering Journal*, vol. 53, no. 3, pp. 723–730, 2014.

[50] M. Devakar, D. Sreenivasu, and B. Shankar, "Analytical solutions of some fully developed flows of couple stress fluid between concentric cylinders with slip boundary conditions," *International Journal of Engineering Mathematics*, vol. 2014, Article ID 785396, 13 pages, 2014.

[51] B. Punnamchandar and Y. S. Fekadu, "Effects of slip and uniform magnetic field on flow of immiscible couple stress fluids in a porous medium channel," *The International Journal of Engineering and Science*, vol. 1, pp. 1–8, 2020.

[52] B. Punnamchandar and Y. S. Fekadu, "Effects of slip and inclined magnetic field on the flow of immiscible fluids (couple stress fluid and Jeffrey fluid) in a porous channel," *Journal of Applied Mathematics*, vol. 2022, Article ID 2799773, 11 pages, 2022.

[53] R. R. Gold, "Magnetohydrodynamic pipe flow. part 1," *Journal of Fluid Mechanics*, vol. 13, no. 4, pp. 505–512, 1962.

[54] C. L. M. H. Navier, "Memoirs de l'Academie," *Royale des Sciences de l'Institut de France*, vol. 1, pp. 414–416, 1823.